Tropical origins of the Pacific meridional mode associated with the nonlinear interaction of ENSO with the annual cycle

F. Jiang, W. J. Zhang, Julien Boucharel, F. F. Jin

Geophysical Research Letters

RESEARCH LETTER
10.1029/2023GL106225

Key Points:

- The spatiotemporal features of Pacific Meridional Mode (PMM) on seasonal-to-interannual timescales exhibit a remarkable resemblance with those of the tropical combination mode
- C-mode-related atmospheric anomalies are capable of inducing PMM-like sea surface temperature changes in the tropical Pacific
- El Niño-Southern Oscillation (ENSO)'s interaction with the annual cycle manifests in PMM-related air-sea conditions, which explains the observed ENSO-PMM linkage

Supporting Information:

Supporting Information may be found in the online version of this article.

Correspondence to:

W. Zhang,
zhangwj@nuist.edu.cn

Citation:

Jiang, F., Zhang, W., Boucharel, J., & Jin, F.-F. (2023). Tropical origins of the Pacific Meridional Mode associated with the nonlinear interaction of ENSO with the annual cycle. *Geophysical Research Letters*, *50*, e2023GL106225. https://doi.org/10.1029/2023GL106225

Received 6 SEP 2023
Accepted 29 NOV 2023

Tropical Origins of the Pacific Meridional Mode Associated With the Nonlinear Interaction of ENSO With the Annual Cycle

Feng Jiang[1], Wenjun Zhang[1], Julien Boucharel[2], and Fei-Fei Jin[3]

[1]CIC-FEMD/ILCEC, Key Laboratory of Meteorological Disaster of Ministry of Education (KLME), Nanjing University of Information Science and Technology, Nanjing, China, [2]Université de Toulouse III, LEGOS, (CNRS/IRD/UPS), Toulouse, France, [3]Department of Atmospheric Sciences, School of Ocean and Earth Science and Technology (SOEST), University of Hawai'i at Mānoa, Honolulu, HI, USA

Abstract The Pacific Meridional Mode (PMM) has long been associated with extra-tropical air-sea coupling processes, which are thought to influence the development of El Niño-Southern Oscillation (ENSO). Here we show that the PMM on seasonal to interannual timescales is closely associated with a newly proposed tropical mode known as the ENSO Combination mode (C-mode), which arises from the nonlinear interaction between ENSO and the background annual cycle in the deep tropics. The PMM exhibits a remarkable resemblance with the C-mode in atmospheric patterns, spectral characteristics, and local impacts. Based on a simple Hasselmann-type model, we further demonstrate that the C-mode-related atmospheric anomalies can effectively drive PMM-like sea surface temperature anomalies. As the C-mode captures seasonally modulated ENSO characteristics, the seasonal-to-interannual PMM variability could naturally establish a connection with ENSO, thereby offering an alternative explanation for the observed relationship between PMM and ENSO.

Plain Language Summary Previous studies demonstrated that the Pacific Meridional Mode (PMM) is driven by the extratropical climate systems, which can impact the development of El Niño-Southern Oscillation (ENSO) events in the tropics. In our study, we establish a close connection between the PMM on seasonal-to-interannual timescales and a tropical atmospheric mode arising from the nonlinear interaction between ENSO and the background annual cycle (the ENSO Combination mode, C-mode). The C-mode closely resembles the PMM in terms of atmospheric patterns and spectral characteristics. We further demonstrate that the C-mode could drive a PMM-like SST pattern in the tropical Pacific. Consequently, we suggest that the PMM on seasonal-to-interannual timescales has tropical origins, thereby offering an alternative explanation for the relationship between the conventional PMM index and the mature phase of ENSO.

1. Introduction

The tropical meridional mode was first discovered over the tropical Atlantic region (Chang et al., 1997; Nobre & Shukla, 1996), the Atlantic Meridional Mode (AMM), where it dominates the atmosphere-ocean variability on interannual to decadal timescales. This mode exhibits anomalous sea surface temperature (SST) anomalies of opposite sign north and south of the equator, accompanied by cross-gradient wind anomalies directed from cold to warm SST anomalies. In the tropical Pacific, the meridional mode was thought to be less important due to the local dominance of El Niño Southern Oscillation (ENSO) (Wallace et al., 1998). By isolating the variability that is independent of concurrent ENSO conditions (Chiang & Vimont, 2004), first identified the Pacific Meridional Mode (PMM), which is characterized by warm SST anomalies extending southwest from the California coast into the equatorial central Pacific and cold SST anomalies in the eastern equatorial Pacific during its positive phase (see Figure 1a). The PMM exhibits a pronounced similarity with the AMM in terms of its spatial pattern, seasonality and possible connection to the extratropical climate system (Chiang & Vimont, 2004; Vimont et al., 2001, 2003). In particular, the PMM was first argued to be driven by the North Pacific Oscillation (NPO) (Vimont et al., 2001, 2003), parallel to the influence of the North Atlantic Oscillation (NAO) on the AMM through the wind-evaporation-SST (WES) feedback process (Nobre & Shukla, 1996; S.-Ping. Xie & Philander, 1994).

The study of PMM has received considerable attention in recent years, mainly due to its potential as a predictive signal for the onset and development of ENSO events (Alexander et al., 2010; Amaya, 2019; Chang et al., 2007;

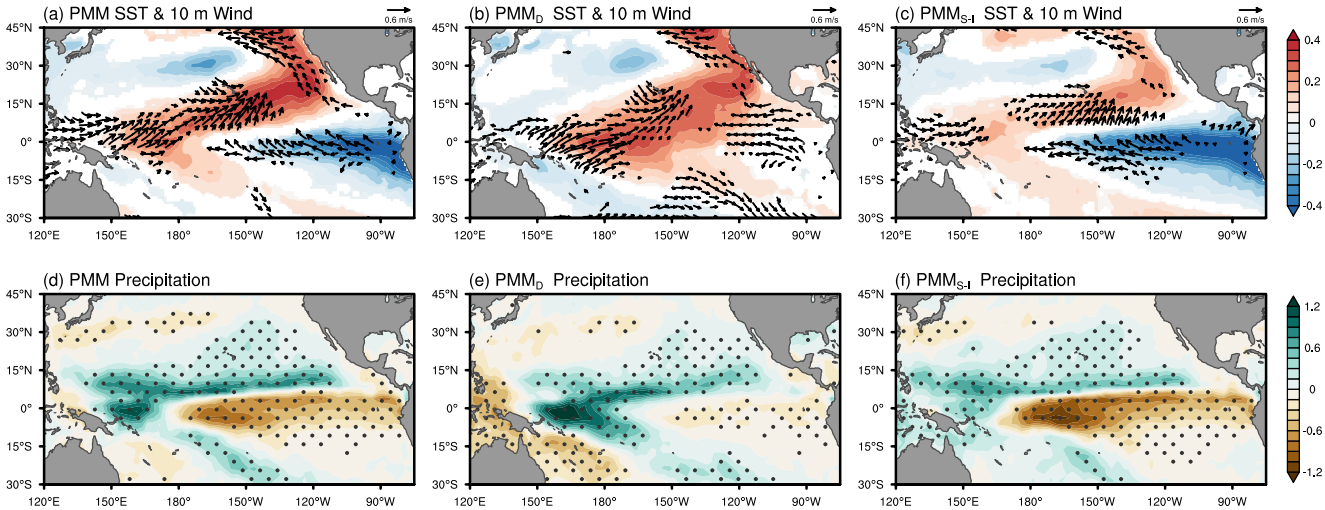

Figure 1. SST (shading; ℃) and 10 m wind (vectors; m/s) anomalies regressed on the (a) the PMM index, (b) the PMM index on decadal timescales (PMM$_D$) and (c) the PMM index on the seasonal-to-interannual timescales (PMM$_{S-I}$). Only regression coefficients for SST that exceed the 95% confidence tests are shown, along with vectors that pass the 95% significance test in either the zonal or meridional component. (d–f) Similar to (a–c) but for precipitation anomalies. Dots indicate values exceeding the 95% significance test.

Geng et al., 2023; S. Larson & Kirtman, 2013; S. M. Larson & Kirtman, 2014). Various physical processes have been proposed to explain the pathway by which the PMM influences ENSO, including the seasonal footprinting mechanism (Chiang & Vimont, 2004; Vimont et al., 2001, 2003), the trade wind charging process (Anderson et al., 2013), and the summer deep convection triggering mechanism (Amaya, 2019; Amaya et al., 2019). However, recent studies suggest that the PMM, which was a previously widely-recognized conduit for extra-tropical atmospheric variabilities to impact ENSO, actually has tropical origins (Richter et al., 2022; Stuecker, 2018; H. Zhang, Deser, et al., 2014; Y. Zhang et al., 2022).

The complexity and uncertainty of the PMM dynamics as well as its relationship with tropical Pacific variability can be attributed, in part, to its wide spectrum ranging from seasonal to decadal timescales. Previous studies have noted the close agreement between the low-frequency component of the PMM and tropical central Pacific decadal variability, yet whether mid-latitude dynamics are essential in enabling such a linkage on decadal timescales remains debated (Di Lorenzo et al., 2015; Joh & Di Lorenzo, 2019; C. Liu et al., 2019; Richter et al., 2022; Stuecker, 2018; Wu et al., 2021). On shorter timescales, the PMM is frequently linked to the stochastic atmospheric forcing in the mid-latitudes (Vimont et al., 2001, 2003). For example, previous studies suggest that the circulation anomalies associated with the southern lobe of the NPO could modulate the intensity of local trade wind and produce surface latent heat flux anomalies, thereby contributing to SST variations resembling the PMM (Chang et al., 2007; Joh & Di Lorenzo, 2019; Vimont et al., 2003). In contrast, Stuecker (2018) demonstrated that the high-frequency component of PMM exhibits a strong instantaneous relationship with the central Pacific ENSO. However, it is noted that this finding was based on the PMM index which does not exclude the influence of ENSO. At present, the mechanisms for the PMM variability on seasonal-to-interannual timescales remain not clear.

In this study, we focus on the dynamics of the seasonal-to-interannual component of PMM variability and its relationship with the tropical air-sea processes. Our analysis reveals a strong association between PMM variability on this timescale and the ENSO Combination mode (C-mode), which arises from nonlinear interactions with the background SST annual cycle. Given that the C-mode captures the ENSO characteristics modulated by the background annual cycle, the connection between the PMM variability and ENSO on seasonal-to-interannual timescales is naturally established, which provides an alternative explanation for the observed linkage between extra-tropical variability and tropical ENSO on seasonal-to-interannual timescales.

2. Methods

Anomalies for all variables were calculated as the departures from the monthly mean climatology and the linear trend was removed to avoid possible influence of global warming. Statistical significance tests were conducted

based on the two-tailed Student's *t*-test with effective degrees of freedom ($N_{eff} = N/\tau_n$). Here N denotes the sample size and $\tau_n = \sum_{i=-\infty}^{i=\infty} R_1(i)R_2(i)$, where $R_1(i)$ and $R_2(i)$ are the autocorrelation of two sample series at the lag time of i, respectively (Davis, 1976). The PMM index used is provided by the University of Wisconsin-Madison, which is derived by applying Maximum Covariance Analysis (MCA) to SST and the zonal and meridional components of the 10-m wind field over the region of 21°S–32°N, 74°W–15°E (Amaya, 2019). Noted that the ENSO-related variability is subtracted before the MCA is applied. Here the PMM index is derived by projecting SST data onto the spatial structure yielded by the MCA. The Niño 3.4 index was calculated as SST anomalies averaged over 5°S–5°N, 120°–170°W. ENSO events were defined based on a threshold of ±0.5°C of the Niño 3.4 index in boreal winter (November to January). Eleven El Niño (1982, 1986, 1987, 1991, 1994, 1997, 2002, 2004, 2009, 2014, 2015, 2018, and 2019) and fourteen La Niña (1983, 1984, 1985, 1988, 1995, 1998, 1999, 2000, 2005, 2007, 2018, 2010, 2011, and 2017) events were identified. The El Niño events of 1982, 1997, and 2015 are classified as strong El Niño events while the other events are referred to as moderate ENSO events. The NiñoA index is defined following W. Zhang et al. (2016) to characterize the meridional asymmetry of ENSO.

3. Results

3.1. PMM on Seasonal-To-Interannual Timescales and Its Linkage With ENSO

We first regressed the surface wind, SST, and precipitation anomalies on the unfiltered PMM index (Figures 1a and 1d). The PMM in its positive phase features warm SST anomalies extending from the subtropical northeastern Pacific into the equatorial central Pacific and cold anomalies in the eastern Pacific. This SST anomaly pattern is accompanied by southwesterlies extending from the western-to-central Pacific to the subtropical northeastern Pacific and easterlies in the eastern Pacific. Previous studies have revealed a prominent decadal component in the PMM besides the interannual component (C. Liu et al., 2019; Stuecker, 2018), which is also evident in the spectrum of the PMM index. Considering that diverse mechanisms may be at play on different timescales, we separate the PMM variabilities into seasonal-to-interannual (<8 yr; $PMM_{S\text{-}I}$) and decadal (>8 yr; PMM_D) components based on the Fast Fourier Transform filtering method.

The PMM on decadal timescales is characterized by meridionally broad horseshoe patterns of central Pacific El Niño-like SST anomalies (Figure 1b). These positive SST anomalies in the central Pacific are accompanied by pronounced westerly wind anomalies and positive precipitation anomalies in the western Pacific (Figures 1b and 1e). The PMM has been shown to have a strong coherence with tropical central Pacific SST variability on decadal timescales, although their causal relationship remains a subject of ongoing debate (E. Di Lorenzo et al., 2015; Stuecker, 2018). On the seasonal to interannual timescale, the equatorial loadings of PMM SST anomalies demonstrate relatively stronger magnitudes compared to the northern hemisphere, with a more pronounced meridional asymmetry than observed on decadal timescales (Figure 1c). The PMM on seasonal-to-interannual timescales is associated with an anomalous precipitation pattern featuring a robust asymmetric meridional component, which is more prominent compared to its zonal counterpart (Figure 1f).

As shown in Figure 2a, the PMM exhibits a significant spectral peak around 0.67 yr^{-1}, in addition to the interannual peak around 0.25 yr^{-1} and the quasi-decadal peak around 0.1 yr^{-1}. Interestingly, this spectral peak of the PMM index coincides with that of the Niño 3.4 index. The Niño 3.4 index displays concentrated power on seasonal-to-interannual timescales, featuring prominent interannual peaks ranging from 0.2 to 0.5 yr^{-1} (Stein et al., 2014). Besides, a robust peak around 0.7 yr^{-1} is also evident, which has been explained as resulting from the interaction between ENSO and the background annual cycle (Stuecker et al., 2013), a signature of the seasonally modulated ENSO variability. Notably, the PMM on seasonal-to-interannual timescales displays also a distinct peak of variability around January, in contrast to the flat seasonal variance structure observed for the unfiltered PMM index, which peaks from late winter to early summer seasons (Figures 2b and 2c).

To further illustrate the relationship between PMM and ENSO on seasonal-to-interannual timescales, we further display in Figure 2d the time series of $PMM_{S\text{-}I}$ and Niño 3.4 index. Here we do not conduct the high-pass filtering on the Niño 3.4 index, considering its less prominent decadal component (Figures 2a–2c). While the orthogonality of the PMM and ENSO is dictated by mathematical constraints, the $PMM_{S\text{-}I}$ exhibits a moderate simultaneous correlation with ENSO ($R = -0.3$, significant at the 95% significance level) and the PMM on decadal timescales shows high coherence with tropical central Pacific quasi-decadal SST variability (C. Liu et al., 2019; Stuecker, 2018). Moreover, the same-signed PMM events are often observed to precede

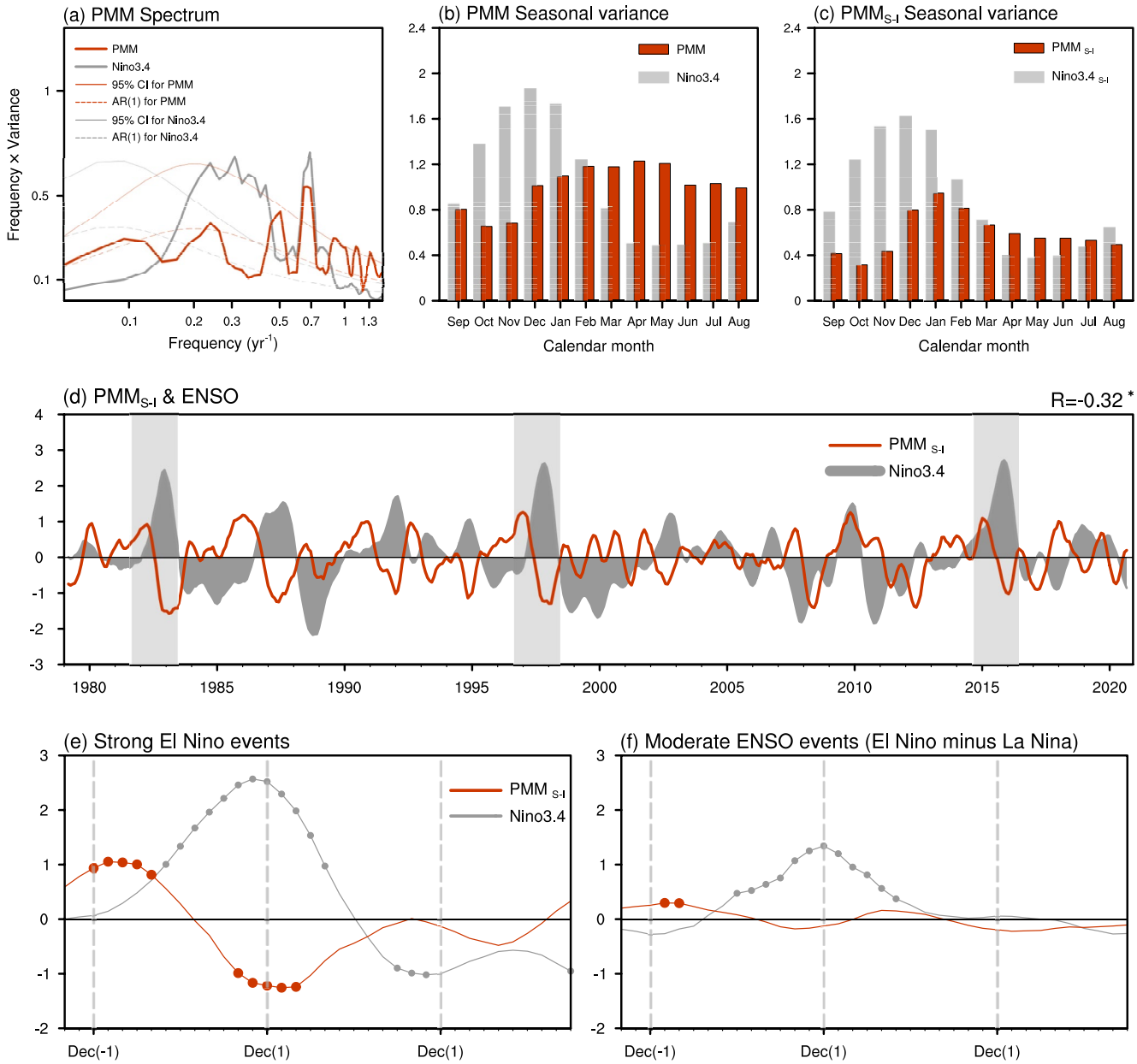

Figure 2. (a) Spectrum for the PMM index (thick red line) and Niño 3.4 index (thick gray line). Solid thin line and dashed thin line indicate the 95% confidence interval and red noise test for the PMM index (red) and Niño 3.4 index (gray line), respectively. (b) Monthly variance of Niño 3.4 index (gray bar) and PMM index (red bar). (c) Monthly variance of the Niño 3.4 index (gray bar) PMM index (red bar) on the seasonal-to-interannual timescale. (d) Time series of 6-month running mean PMM_{S-I} index (red line) and Niño 3.4 index (dark gray shading). Light gray shadings indicate three strong El Niño events. The correlation between the two indices is also displayed with asterisks (*) indicating values that exceed the 95% confidence test. (e) Time evolution of 6-month running mean PMM_{S-I} (red line) and Niño 3.4 index (gray line) during strong El Niño events. (f) Time evolution of 6-month running mean PMM_{S-I} index (red line) and Niño 3.4 index (gray line) during moderate ENSO events (half the difference between moderate El Niño events and La Niña events). Dots in (e) and (f) indicate values exceeding 95% significance test.

ENSO events, while opposite-signed PMM events occur during the mature and decaying phase of ENSO. This phase relationship is particularly prominent during strong El Niño events, such as those observed in 1982, 1997, and 2015 (Figure 2e). For other ENSO events, the phase relationship appears to be relatively weak (Figure 2f). The locked behavior of PMM_{S-I} with the ENSO lifecycle, especially during strong El Niño events, again suggests the close linkage between ENSO and PMM variability on seasonal to interannual timescales.

3.2. PMM and ENSO Combination Mode (C-Mode)

Previous studies have shown that ENSO-related SST anomalies could establish an effective interaction with the background warm pool SST seasonal cycle, resulting in the generation of an ENSO Combination mode (C-mode) (Stuecker et al., 2013, 2015; W. Zhang et al., 2015). The C-mode has first been proposed as the second empirical orthogonal function (EOF) mode of the tropical Pacific surface wind anomalies (Stuecker et al., 2013). It features a pronounced meridional asymmetric circulation structure with southward-shifted westerly anomalies over the central equatorial Pacific and anticyclonic anomalies over the western North Pacific, while the first EOF mode (i.e., ENSO mode) exhibits equatorially quasi-symmetric westerly anomalies over the central-to-eastern Pacific. The C-mode also manifests itself in the tropical precipitation fields, featuring a meridional dipole of tropical rainfall variability that spans asymmetrically across the equator, which is also known as the Pacific precipitation dipole mode (PPDM) (Fukuda et al., 2021). Through a multi-variate EOF analysis on the equatorial Pacific (5°S–5°N, 150°E–85°W) precipitation and surface wind anomalies, we can identify a meridional quasi-symmetric atmospheric mode (Figure 3a) and a meridionally asymmetric atmospheric mode (Figure 3b). The quasi-symmetric atmospheric mode is closely linked to ENSO and their correlation reaches as high as 0.94 (significant at the 95% significance level; Figure 3c). The dynamical aspects of the tropical atmospheric meridional mode align with the previously identified C-mode based on wind fields and the PPDM based on precipitation fields, revealing a strong connection with the nonlinear interaction between ENSO and the annual cycle (Figures S1 and S2 in Supporting Information S1), and we hereafter refer to the tropical atmospheric meridional mode as C-mode for simplicity.

As shown in Figures 1f and 3b, the C-mode-related atmospheric pattern exhibits a striking resemblance to that of $PMM_{S\text{-}I}$, both featuring a meridional asymmetrical structure with opposite-signed wind and precipitation anomalies over the northern and southern off-equatorial Pacific. And the time series of PMM is significantly related to the C-mode ($R = -0.56$, significant at the 95% confidence level). In particular, the phase reversal of the PMM during strong El Niño events (Figure 2e) is consistent with that observed in the seasonal evolution of C-mode during these events (Figure 3d). As elaborated in previous studies, the phase change of C-mode during the ENSO lifecycle holds a clear physical meaning (Fukuda et al., 2021; Stuecker et al., 2013, 2015; W. Zhang et al., 2015). The C-mode comes from the nonlinear air-sea interaction between ENSO and the background annual cycle, mainly capturing the ENSO-related tropical meridional displacement of convection due to the seasonal migration of the background warm pool. As a result, the C-mode signal is distinctly detectable in atmospheric anomalies, such as surface wind (Stuecker et al., 2013) and convection (Fukuda et al., 2021).

Considering the close connection between the atmospheric pattern associated with the PMM and that of the C-mode, it is reasonable to infer that the above seasonal modulation of ENSO events by the background annual cycle is also manifested in atmospheric fields related to the PMM. In fact, the phase relationship between PMM and ENSO (Figures 2e and 2f) closely resembles that between C-mdoe and ENSO (Figure S3 in Supporting Information S1), especially during strong El Niño events. Next, we show that the C-mode-related atmospheric anomalies could drive PMM-like SST anomalies. The C-mode signal cannot be directly detected in the EOF analyses of SST anomalies, possibly related to the reddening effects due to air–sea interaction process (Stuecker et al., 2013, 2015). Compared to the fast-varying atmosphere system that is dominated by short-timescale variability, the ocean system tends to exhibit longer-timescale variability ranging from interannual to decadal timescales with increased power at low frequencies and decreased power at high frequencies (Frankigoul & Hasselmann, 1977). Nevertheless, the C-mode-related atmospheric anomalies are capable of driving the SST anomaly change via anomalous atmospheric forcing in the following months (W. Zhang et al., 2016). To obtain the SST anomaly pattern forced by the C-mode, we establish a simple Hasselmann-type equation (Frankignoul & Hasselmann, 1977; Hasselmann, 1976; W. Zhang et al., 2016):

$$\frac{dT_C}{dt} = -\lambda T_C + \beta C$$

where T_C represents the SST variability driven by the C-mode-related atmospheric anomalies, λ is the damping rate, β is the forcing rate, and C is the normalized PC2 related to the atmospheric forcing associated with the C-mode. Here λ is estimated as $\frac{1}{30}$ day^{-1} and β is estimated as $\frac{1}{60}$ day^{-1} to roughly characterize the local air-sea sensitivity following W. Zhang et al. (2016). It is essential to note that this equation focuses solely on thermodynamics and does not consider the role of ocean dynamics. Then the C-mode related SST spatial pattern

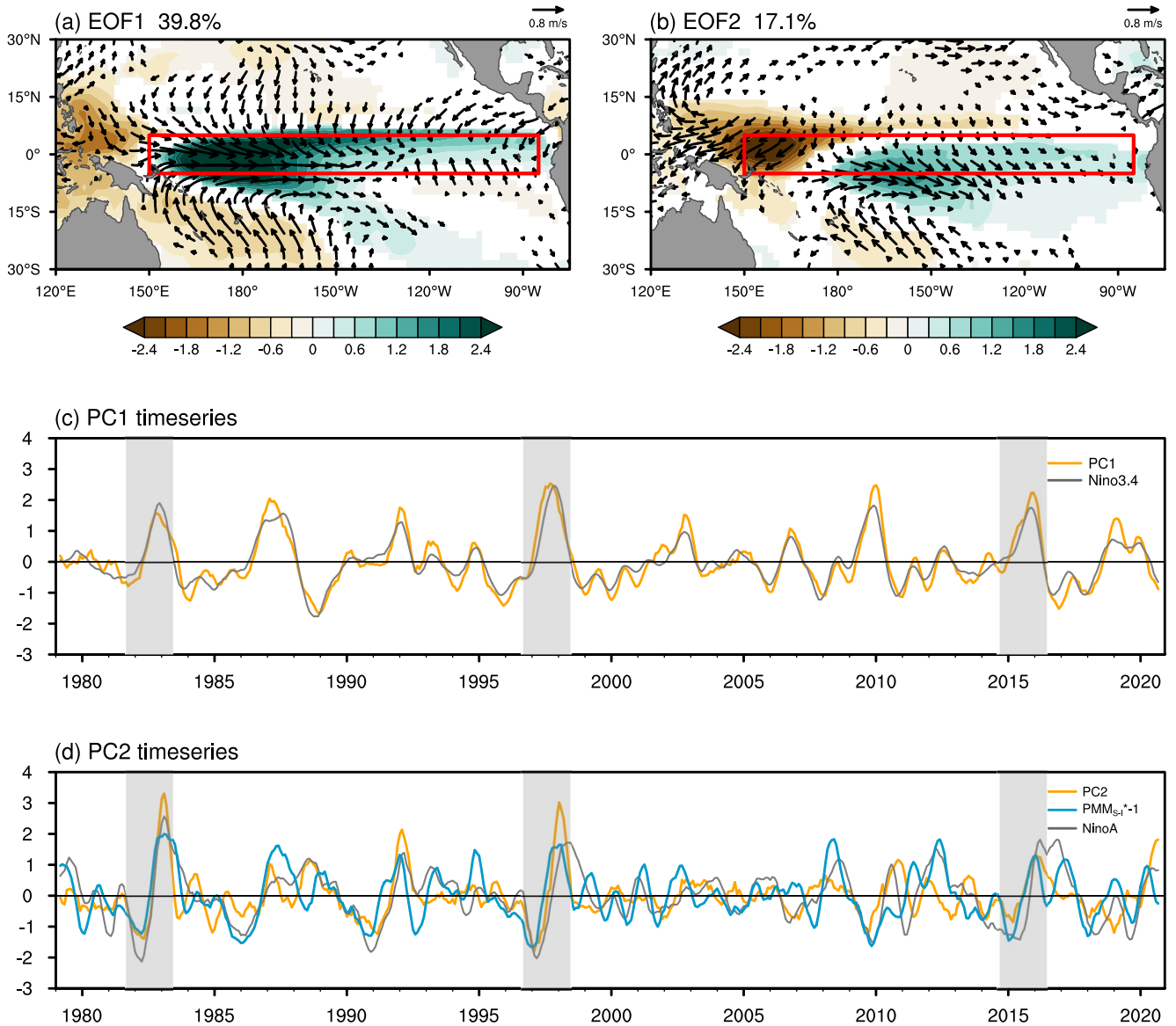

Figure 3. (a) and (b) Spatial patterns of the two leading MV-EOF modes for tropical surface wind and precipitation anomalies obtained by linear regression of the surface wind (vectors; m/s) and precipitation anomalies (shading; mm/day) on the corresponding normalized principal components. Precipitation regression coefficients that pass the 95% confidence tests are displayed, along with vectors that pass the 95% significance test in either the zonal or meridional components. The explained variance of the leading two modes is also displayed. (c) Normalized 6-month running mean first principal component (PC1) and Niño 3.4 index; (d) Normalized 6-month running mean second principal component (PC2) (orange line), PMM_{S-I} (blue line, shown with a factor of −1 for display) and Niño A index (gray line). Light gray shadings in (c) and (d) indicate three strong El Niño events.

can be obtained by regressing the SST anomaly upon T_C (Figure S4 in Supporting Information S1). The SST anomaly pattern related to the C-mode (Figure S4 in Supporting Information S1) is similar to that related to PMM_{S-I} (Figure 1c), both featuring SST anomalies of opposite signs in the eastern equatorial to southern tropical Pacific and the subtropical regions of the north and south Pacific. Notably, the subtropical loadings associated with the PMM_{S-I} are mainly located in the northern hemisphere, whereas those associated with the C-mode are also prominent across the western equatorial Pacific and southern subtropical Pacific—exhibiting a more extensive basin-scale pattern encompassing the South Pacific Meridional Mode (SPMM, H. Zhang, Clement, & Di Nezio, 2014).

We further compare the seasonal evolution of air-sea anomalies related to the PMM_{S-I} with those associated with the C-mode by performing lead-lag regressions of surface wind and SST anomalies onto the PMM_{S-I} index during its peak seasons (December-January-February-March) and those of C-mode-driven SST (T_C index). As shown

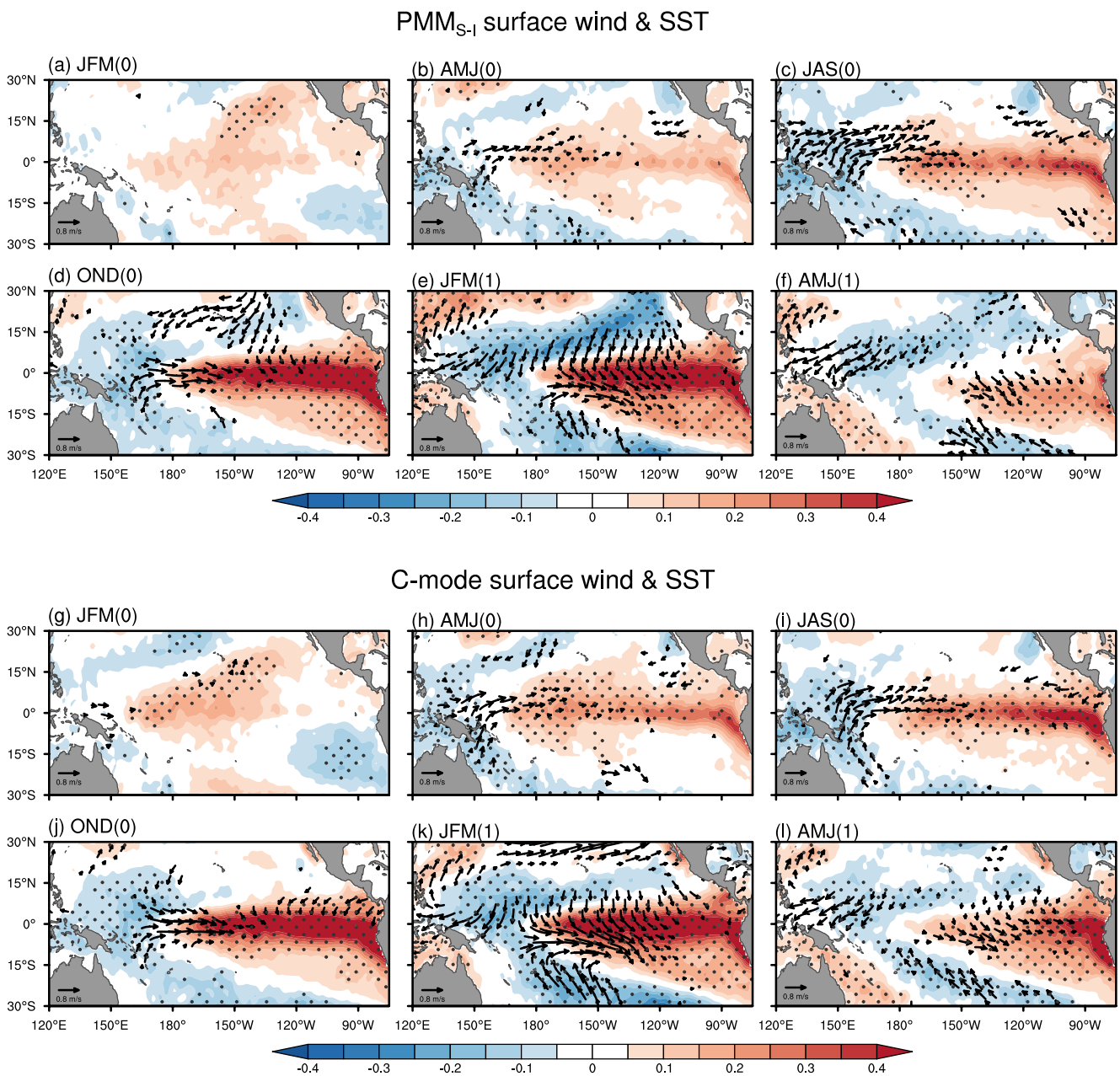

Figure 4. (a)–(f) Surface wind and SST anomalies in January-February-March(0) (JFM(0)), April-May-June(0) (AMJ(0)), July-August-September(0) (JAS(0)), October-November-December(0) (OND(0)), January-February-March(1) (JFM(1)), and April-May-June(1) (AMJ(1)) regressed onto December(0)-January-February-March(1) (D(0)JFM(1)) PMM$_{S-I}$ index (multiplied by a factor of −1 for comparison). (g)–(l) Similar to (a)–(f) but for surface wind anomalies regressed onto D(0)JFM(1) C-mode index and SST anomalies regressed onto D(0)JFM(1) C-mode driven SST (T_C). Numerals "0" and "1" represent the previous and concurrent years, respectively. Dots indicate regression anomalies for SST exceeding 95% significance test. Vectors exceeding the 95% statistical significance in either the zonal or meridional components are displayed.

Figure 4, the seasonal evolutions of air-sea anomalies associated with PMM$_{S-I}$ exhibit a close resemblance to those of the C-mode. The air-sea anomalies associated with the C-mode predominantly represent the meridionally asymmetrical aspects of ENSO throughout its entire lifecycle (Figures 4g–4l) (Stuecker et al., 2013; W. Zhang et al., 2016). During the early spring of El Niño developing year, the C-mode related SST anomalies are characterized with positive SST anomalies in the central Pacific extending into the subtropical North Pacific, along with negative SST anomalies south of the equator. These anomalies are likely a consequence of the ENSO transition from a La Niña-like state to an El Niño-like state. For example, as shown in Figures S5a and S5b in Supporting Information S1, the SST anomalies in tropical Pacific during early springs of 1982 and 1997 feature a distinct

horseshoe-shaped SST anomaly pattern, accompanied by strong easterly winds in the off-equatorial region of the southern hemisphere and cyclonic circulation anomalies in the western North Pacific. This air-sea anomaly pattern (Figures 4g and 4h) could then project onto the PMM pattern (Figures 4a and 4b). During the developing summer-fall season, when the Pacific Intertropical Convergence Zone is positioned in the northern hemisphere, the quasi-symmetric El Niño-related SST anomalies with respect to the equator are accompanied with surface wind anomalies which are located near and north of the equator in the central-to-western Pacific. Figures 4e and 4k show the near-simultaneous patterns of air-sea variabilities that are related to $PMM_{S\text{-}I}$ and C-mode, respectively, which are similar to the monthly regression (Figure 1c and Figure S4 in Supporting Information S1). Subsequently, during the El Niño decaying spring when the South Pacific Convergence zone strengthens, there appears a strong southward displacement of El Niño-related westerly anomalies (Figures 4j–4l). Due to ENSO-driven interhemispheric Pacific mass transports (McGregor et al., 2012), the meridional dipole of atmospheric anomalies changes its sign after the peak of ENSO, which also results in a strong projection of air-sea anomalies onto the PMM pattern (Figures 4d–4f). While we cannot rule the possibility that the strong PMM anomalies during the decaying spring of strong El Niño might be a mathematical projection of tropical SST anomalies onto the PMM pattern (Fan et al., 2023), rather than being a consequence of ENSO's prevalence over the subtropical Pacific (Stuecker, 2018), the above analysis clearly reveal that a substantial portion of PMM as reflected by the $PMM_{S\text{-}I}$ index originates from the deep tropics due to the nonlinear interaction between tropical ENSO and the background annual cycle.

4. Summary and Discussion

This study documents a close relationship between the PMM on seasonal to interannual timescales and a tropical atmospheric meridional mode arising from the nonlinear interaction between ENSO and the annual cycle. The effective interaction between ENSO and the annual cycle could give rise to a PMM-like pattern in atmospheric and oceanic fields including SST, surface wind, and precipitation. Thus, we proposed that the air-sea anomalies associated with PMM on seasonal to interannual timescales, as indicated by the conventional PMM index, exhibit significant origins from tropical regions. Considering that the tropical atmospheric meridional mode captures the seasonal modulation of ENSO by the background annual cycle, the seasonal-to-interannual PMM variability could naturally arise from a similar connection with ENSO. This result provides an alternative explanation for the relationship between the conventional PMM index and the mature phase of ENSO, offering new insights into the complex dynamics between these phenomena.

Considering the close connection of PMM with the climate mode in the deep tropics, there might be a substantial overlap in the explanation of Pacific-rim climate variability by the extra-tropical or tropical climate systems in previous studies. Notably, the PMM has been widely used as a key contributing factor in understanding East Asian climate variations, including extreme precipitation and landfall typhoon events (Gao et al., 2018; Z. Liu et al., 2021). Nonetheless, other studies have shown that a significant portion of the variability of the East Asian Summer Monsoon can be adequately understood by focusing solely on the ENSO and its interaction with the background annual cycle (Stuecker et al., 2015; W. Zhang et al., 2016). In particular, W. Zhang et al. (2016) introduced the Niño-A index to capture the tropical C-mode-related SST variability, which effectively captures both equatorial and off-equatorial SST anomalies throughout the ENSO lifecycle and also depicts a robust year-round ENSO/monsoon relationship and the summer flooding occurrences in the Yangtze River basin. Interestingly, we have observed a remarkably high coherence between the Niño-A index and $PMM_{S\text{-}I}$ index (Figure 3d). Nevertheless, an alternative explanation arises from the fact that, while the C-mode is defined as the EOF2 of equatorial Pacific surface wind and precipitation in the equatorial Pacific, it inherently encompasses other climate signals or noise beyond the nonlinear interaction between ENSO and the annual cycle. In some particular ENSO events like 2015 El Niño (Figures S5c and S5f in Supporting Information S1), the extra-tropical forcing in the North Pacific may play a role in the developing stage (Bond et al., 2015; Di Lorenzo & Mantua, 2016; Santoso et al., 2017), potentially imprinting the C-mode index characterized by the PC2 (Figure 3d). Further investigation is necessary to disentangle the influences of extra-tropical processes on the observed climate variability in the Pacific region.

Data Availability Statement

The global sea ice and SST analysis from the Hadley Centre (HadISST) provided by the Met Office Hadley Centre (Rayner, 2003) is used in this study. The precipitation data from the global precipitation product from the Climate Prediction Center Merged Analysis of Precipitation (CMAP) (P. Xie & Arkin, 1997) are utilized to investigate ENSO-related precipitation impacts. To examine the variation of ENSO-related wind anomalies, we

use monthly 10-m winds from the National Centers for Environmental Prediction–National Center for Atmospheric Research (NCEP–NCAR) reanalysis data set (Kalnay et al., 1996). The PMM index used is provided by the University of Wisconsin-Madison (Chiang & Vimont, 2004).

Acknowledgments
This work was supported by the National Nature Science Foundation of China (42125501).

References

Alexander, M. A., Vimont, D. J., Chang, P., & Scott, J. D. (2010). The impact of extratropical atmospheric variability on ENSO: Testing the seasonal footprinting mechanism using coupled model experiments. *Journal of Climate*, *23*(11), 2885–2901. https://doi.org/10.1175/2010JCLI3205.1

Amaya, D. J. (2019). The Pacific meridional mode and ENSO: A review. *Current Climate Change Reports*, *5*(4), 296–307. https://doi.org/10.1007/s40641-019-00142-x

Amaya, D. J., Kosaka, Y., Zhou, W., Zhang, Y., Xie, S.-P., & Miller, A. J. (2019). The North Pacific pacemaker effect on historical ENSO and its mechanisms. *Journal of Climate*, *32*(22), 7643–7661. https://doi.org/10.1175/JCLI-D-19-0040.1

Anderson, B. T., Perez, R. C., & Karspeck, A. (2013). Triggering of El Niño onset through trade wind-induced charging of the equatorial Pacific: Trade wind charging of the equatorial Pacific. *Geophysical Research Letters*, *40*(6), 1212–1216. https://doi.org/10.1002/grl.50200

Bond, N. A., Cronin, M. F., Freeland, H., & Mantua, N. (2015). Causes and impacts of the 2014 warm anomaly in the NE Pacific. *Geophysical Research Letters*, *42*(9), 3414–3420. https://doi.org/10.1002/2015GL063306

Chang, P., Ji, L., & Li, H. (1997). A decadal climate variation in the tropical Atlantic Ocean from thermodynamic air-sea interactions. *Nature*, *385*(6616), 516–518. https://doi.org/10.1038/385516a0

Chang, P., Zhang, L., Saravanan, R., Vimont, D. J., Chiang, J. C. H., Ji, L., et al. (2007). Pacific meridional mode and El Niño-Southern Oscillation: Pacific meridional mode and ENSO. *Geophysical Research Letters*, *34*(16), L16608. https://doi.org/10.1029/2007GL030302

Chiang, J. C. H., & Vimont, D. J. (2004). Analogous Pacific and Atlantic meridional modes of tropical atmosphere–ocean variability. *Journal of Climate*, *17*(21), 4143–4158. https://doi.org/10.1175/JCLI4953.1

Davis, R. E. (1976). Predictability of sea surface temperature and sea level pressure anomalies over the North Pacific Ocean. *Journal of Physical Oceanography*, *6*(3), 249–266. https://doi.org/10.1175/1520-0485(1976)006<0249:POSSTA>2.0.CO;2

Di Lorenzo, E., Liguori, G., Schneider, N., Furtado, J. C., Anderson, B. T., & Alexander, M. A. (2015). ENSO and meridional modes: A null hypothesis for Pacific climate variability. *Geophysical Research Letters*, *42*(21), 9440–9448. https://doi.org/10.1002/2015GL066281

Di Lorenzo, E., & Mantua, N. (2016). Multi-year persistence of the 2014/15 North Pacific marine heatwave. *Nature Climate Change*, *6*(11), 1042–1047. https://doi.org/10.1038/nclimate3082

Fan, H., Yang, S., Wang, C., & Lin, S. (2023). Revisiting the impacts of tropical Pacific SST anomalies on the Pacific meridional mode during the decay of strong eastern Pacific El Niño events. *Journal of Climate*, *36*(15), 4987–5002. https://doi.org/10.1175/JCLI-D-22-0342.1

Frankignoul, C., & Hasselmann, K. (1977). Stochastic climate models, Part II Application to sea-surface temperature anomalies and thermocline variability. *Tellus*, *29*(4), 289–305. https://doi.org/10.3402/tellusa.v29i4.11362

Fukuda, Y., Watanabe, M., & Jin, F. (2021). Mode of precipitation variability generated by coupling of ENSO with seasonal cycle in the tropical Pacific. *Geophysical Research Letters*, *48*(16), e2021GL095204. https://doi.org/10.1029/2021GL095204

Gao, S., Zhu, L., Zhang, W., & Chen, Z. (2018). Strong modulation of the pacific meridional mode on the occurrence of intense tropical cyclones over the western North Pacific. *Journal of Climate*, *31*(19), 7739–7749. https://doi.org/10.1175/JCLI-D-17-0833.1

Geng, T., Jia, F., Cai, W., Wu, L., Gan, B., Jing, Z., et al. (2023). Increased occurrences of consecutive La Niña events under global warming. *Nature*, *619*(7971), 774–781. https://doi.org/10.1038/s41586-023-06236-9

Hasselmann, K. (1976). Stochastic climate models Part I. Theory. *Tellus*, *28*(6), 473–485. https://doi.org/10.3402/tellusa.v28i6.11316

Joh, Y., & Di Lorenzo, E. (2019). Interactions between Kuroshio extension and central tropical Pacific lead to preferred decadal-timescale oscillations in Pacific climate. *Scientific Reports*, *9*(1), 13558. https://doi.org/10.1038/s41598-019-49927-y

Kalnay, E., Kanamitsu, M., Kistler, R., Collins, W., Deaven, D., Gandin, L., et al. (1996). The NCEP/NCAR 40-year reanalysis project. *Bulletin of the American Meteorological Society*, *77*(3), 437–471. https://doi.org/10.1175/1520-0477(1996)077<0437:TNYRP>2.0.CO;2

Larson, S., & Kirtman, B. (2013). The Pacific meridional mode as a trigger for ENSO in a high-resolution coupled model: Pacific meridional mode and ENSO. *Geophysical Research Letters*, *40*(12), 3189–3194. https://doi.org/10.1002/grl.50571

Larson, S. M., & Kirtman, B. P. (2014). The Pacific meridional mode as an ENSO precursor and predictor in the North American multimodel ensemble. *Journal of Climate*, *27*(18), 7018–7032. https://doi.org/10.1175/JCLI-D-14-00055.1

Liu, C., Zhang, W., Stuecker, M. F., & Jin, F. (2019). Pacific meridional mode-western North Pacific tropical cyclone linkage explained by tropical Pacific Quasi-Decadal variability. *Geophysical Research Letters*, *46*(22), 13346–13354. https://doi.org/10.1029/2019GL085340

Liu, Z., Gao, T., Zhang, W., & Luo, M. (2021). Implications of the Pacific meridional mode for summer precipitation extremes over China. *Weather and Climate Extremes*, *33*, 100359. https://doi.org/10.1016/j.wace.2021.100359

McGregor, S., Timmermann, A., Schneider, N., Stuecker, M. F., & England, M. H. (2012). The effect of the South Pacific convergence zone on the termination of El Niño events and the meridional asymmetry of ENSO. *Journal of Climate*, *25*(16), 5566–5586. https://doi.org/10.1175/JCLI-D-11-00332.1

Nobre, P., & Shukla, J. (1996). Variations of sea surface temperature, wind stress, and rainfall over the tropical Atlantic and South America. *Journal of Climate*, *9*(10), 2464–2479. https://doi.org/10.1175/1520-0442(1996)009<2464:VOSSTW>2.0.CO;2

Rayner, N. A., Parker, D. E., Horton, E. B., Folland, C. K., Alexander, L. V., Rowell, D. P., et al. (2003). Global analyses of sea surface temperature, sea ice, and night marine air temperature since the late nineteenth century. *Journal of Geophysical Research*, *108*(D14), 4407. https://doi.org/10.1029/2002JD002670

Richter, I., Stuecker, M. F., Takahashi, N., & Schneider, N. (2022). Disentangling the North Pacific meridional mode from tropical Pacific variability. *Npj Climate and Atmospheric Science*, *5*(1), 94. https://doi.org/10.1038/s41612-022-00317-8

Santoso, A., McPhaden, M. J., & Cai, W. (2017). The defining characteristics of ENSO extremes and the strong 2015/2016 El Niño. *Reviews of Geophysics*, *55*(4), 1079–1129. https://doi.org/10.1002/2017RG000560

Stein, K., Timmermann, A., Schneider, N., Jin, F.-F., & Stuecker, M. F. (2014). ENSO seasonal synchronization theory. *Journal of Climate*, *27*(14), 5285–5310. https://doi.org/10.1175/JCLI-D-13-00525.1

Stuecker, M. F. (2018). Revisiting the Pacific meridional mode. *Scientific Reports*, *8*(1), 3216. https://doi.org/10.1038/s41598-018-21537-0

Stuecker, M. F., Jin, F.-F., Timmermann, A., & McGregor, S. (2015). Combination mode dynamics of the anomalous northwest Pacific anticyclone. *Journal of Climate*, *28*(3), 1093–1111. https://doi.org/10.1175/JCLI-D-14-00225.1

Stuecker, M. F., Timmermann, A., Jin, F.-F., McGregor, S., & Ren, H.-L. (2013). A combination mode of the annual cycle and the El Niño/Southern Oscillation. *Nature Geoscience*, *6*(7), 540–544. https://doi.org/10.1038/ngeo1826

Vimont, D. J., Battisti, D. S., & Hirst, A. C. (2001). Footprinting: A seasonal connection between the tropics and mid-latitudes. *Geophysical Research Letters*, *28*(20), 3923–3926. https://doi.org/10.1029/2001GL013435

Vimont, D. J., Wallace, J. M., & Battisti, D. S. (2003). The seasonal footprinting mechanism in the Pacific: Implications for ENSO. *Journal of Climate*, *16*(16), 2668–2675. https://doi.org/10.1175/1520-0442(2003)016<2668:TSFMIT>2.0.CO;2

Wallace, J. M., Rasmusson, E. M., Mitchell, T. P., Kousky, V. E., Sarachik, E. S., & von Storch, H. (1998). On the structure and evolution of ENSO-related climate variability in the tropical Pacific: Lessons from TOGA. *Journal of Geophysical Research*, *103*(C7), 14241–14259. https://doi.org/10.1029/97JC02905

Wu, Q., Zhao, J., Zhan, R., & Gao, J. (2021). Revisiting the interannual impact of the Pacific meridional mode on tropical cyclone genesis frequency in the Western North Pacific. *Climate Dynamics*, *56*(3–4), 1003–1015. https://doi.org/10.1007/s00382-020-05515-9

Xie, P., & Arkin, P. A. (1997). Global precipitation: A 17-year monthly analysis based on gauge observations, satellite estimates, and numerical model outputs. *Bulletin of the American Meteorological Society*, *78*(11), 2539–2558. https://doi.org/10.1175/1520-0477(1997)078<2539:GPAYMA>2.0.CO;2

Xie, S.-P., & Philander, S. G. H. (1994). A coupled ocean-atmosphere model of relevance to the ITCZ in the eastern Pacific. *Tellus A*, *46*(4), 340–350. https://doi.org/10.1034/j.1600-0870.1994.t01-1-00001.x

Zhang, H., Clement, A., & Di Nezio, P. (2014). The South Pacific meridional mode: A mechanism for ENSO-like variability. *Journal of Climate*, *27*(2), 769–783. https://doi.org/10.1175/JCLI-D-13-00082.1

Zhang, H., Deser, C., Clement, A., & Tomas, R. (2014). Equatorial signatures of the Pacific meridional modes: Dependence on mean climate state: Zhang et al.: Role of mean state in PMMs' asymmetry. *Geophysical Research Letters*, *41*(2), 568–574. https://doi.org/10.1002/2013GL058842

Zhang, W., Jin, F., Stuecker, M. F., Wittenberg, A. T., Timmermann, A., Ren, H., et al. (2016). Unraveling El Niño's impact on the East Asian monsoon and Yangtze River summer flooding. *Geophysical Research Letters*, *43*(21), 11375–11382. https://doi.org/10.1002/2016GL071190

Zhang, W., Li, H., Jin, F.-F., Stuecker, M. F., Turner, A. G., & Klingaman, N. P. (2015). The annual-cycle modulation of meridional asymmetry in ENSO's atmospheric response and its dependence on ENSO zonal structure. *Journal of Climate*, *28*(14), 5795–5812. https://doi.org/10.1175/JCLI-D-14-00724.1

Zhang, Y., Yu, S., Amaya, D. J., Kosaka, Y., Stuecker, M. F., Yang, J., et al. (2022). Atmospheric forcing of the Pacific meridional mode: Tropical Pacific-driven versus internal variability. *Geophysical Research Letters*, *49*(7), e2022GL098148. https://doi.org/10.1029/2022GL098148